

ON THE STABILITY OF BIRKELAND CURRENTS

Donald E. Scott

Dept. of Electrical Engineering (Retired), U. of Massachusetts, Amherst, Mass
dascott3@cox.net

Abstract — A description of the major consequences of the Scott/Lundquist (Bessel function) mathematical/physical model of a Force-Free Current (FFC) is presented. A formal, mathematical derivation of this model was published in Progress-in-Physics (2015). The intent here is to present an intuitive understanding of the physical functionality implied by that model. Analysis of the results of the derivation indicates that a complete response of the particles in a moving plasma to its internal Lorentz magnetic forces results in a complex but relaxed, freely formed structure that has robust stability. Perturbations of this resulting steady-state configuration are countered by that same inherent Lorentz magnetic force. Thus there is a built-in, negative-feedback mechanism that exists in the canonical Force-Free (Birkeland) Current structure that enables its being not only a self-organizing, but also, a self-sustaining system.

I. INTRODUCTION

A single, simple question was the genesis of the development of what is called the Bessel function model of a Birkeland Current. That question was:

“Given a plasma (a cloud of positively and negatively charged particles) that is moving freely through cosmic space, into what structural shape (if any) will it form - will it self-organize into some well-defined configuration? Or will it just expand outward and dissipate via unbounded diffusion and/or recombination processes?”

To answer this question, a model of what the charges in the plasma will do naturally, by themselves, if no external forces are applied to them was sought. Before presenting the results of this modeling process, we re-list the assumptions made in its derivation:

- 1) A set of charges (both positive and negative) is in motion. The direction of motion of the center of that charged cloud defines the ‘z-direction’ of travel. Although each particle may experience random movements, the entire cloud is moving collectively in that z-direction.
- 2) No external forces are present that can shape, distort, collide with, or otherwise affect the plasma. The flow is taking place in an isolated, force-free space.
- 3) The fundamental laws of electromagnetism (e.g., Maxwell’s equations) apply.
- 4) There is a finite limit to the total amount of charge. The cloud has a finite but unspecified size. No assumption is made regarding the spatial distribution of charges within the cloud.
- 5) The motion and behavior of each charge within the plasma is independent of its value of z (its particular location along the axis). Similarly there is no dependency on its azimuthal angle, θ (its angular position around that z-axis). In deep space any location along the z-axis is indistinguishable from any

other and similarly, no azimuthal angle, θ , is to be preferred over any other.

Given these assumptions, a cylindrical coordinate system (z, θ, r) was chosen to describe the system.

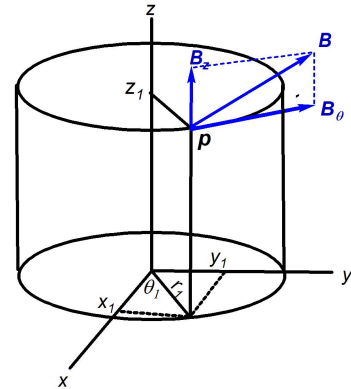


Figure 1 Cylindrical coordinates used to describe any point in a FFC.

Any moving charge constitutes an electric current density vector, \mathbf{j} . Any electric current will produce a magnetic field, \mathbf{B} .

We realize that assumption 5 above dictates that the current density, \mathbf{j} at any given point in our plasma and its associated magnetic field, \mathbf{B} , are each functions only of the radius value, r , of their position. Exactly where the point, p , is located in the z or θ dimensions has no consequence.

Figure 1 shows that the magnetic field strength, \mathbf{B} , at any point, p , in the plasma is made up of two orthogonal unit vector components: \mathbf{B}_z , and \mathbf{B}_θ . At every point in the plasma, the total magnetic-field \mathbf{B} vector is the sum of these two vector components, \mathbf{B}_z , and \mathbf{B}_θ , whose direction angles are defined by (parallel with) the fixed dimensional axes of the cylindrical coordinate system, z and θ . Therefore at every point in the plasma the two component vectors are always perpendicular to each other, but their magnitudes vary independently of each other, depending only on the

value of their radius, r . Similarly, the current density at every point, p , has components j_z and j_θ .

Because the only independent variable in the model is, r , the radial distance out from the z -axis, quantitative descriptions of $B_z(r)$, $B_\theta(r)$, $j_z(r)$, and $j_\theta(r)$ completely define the model.

II. THE LORENTZ FORCE

Any charge moving with respect to a magnetic field will experience a magnetic Lorentz force, and it will respond to that force. It is an inherent force that occurs when a magnetic field vector and a current vector intersect. This force is given as the vector cross-product of the current density, j vector and the magnetic-field vector, B :

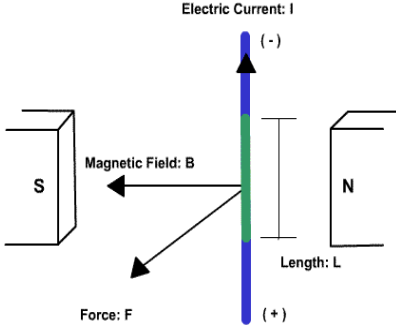


Figure 2 The magnetic Lorentz force.

$f_L = j \times B$. The magnitude of this force is the product of the magnitudes of j and B times the sin of the angle between them. Therefore, if the j vector and the B vector are parallel at point p , the Lorentz force there will be zero-valued.

In the real world, matter will tend to move and/or reconfigure itself if it can, in such a way as to minimize any forces it is experiencing. This is why water flows downhill – the force of gravity is pulling it – the water “goes with the flow”; lightning travels a minimum resistance path – the electric force of the voltage gradient is pulling it; and heat energy follows the descending temperature gradient. If it is assumed that no external forces or barriers are applied to a grouping of positive and negatively charged particles in otherwise free-space, the only force that can shape the flow is the internally generated Lorentz magnetic force between the current density, j vector and the magnetic-field vector B .

III. THE SCOTT/LUNDQUIST MODEL

A system of particles will tend to minimize the effect of any forces it experiences. Converting this word statement into a mathematical expression, and then solving it, results in the set of five defining expressions below [1].

$$B_z(r) = B_z(0)J_0(ar) \quad (1)$$

$$B_\theta(r) = B_z(0)J_1(ar) \quad (2)$$

$$j_z(r) = \frac{\alpha B_z(0)}{\mu} J_0(ar) \quad (3)$$

$$j_\theta(r) = \frac{\alpha B_z(0)}{\mu} J_1(ar) \quad (4)$$

$$B_r(r) = j_r(r) = 0 \quad (5)$$

None of these five quantities are functions of z or θ . They vary **only** with, r , the radial distance of the point of interest from the central z -axis. Therefore every possible value of the independent variable, r , defines a single, virtual cylindrical surface (defined by all the points that have that particular value of r). This virtual cylinder extends for an unlimited distance in the $\pm z$ directions and completely contains (surrounds) the z -axis and all other such cylindrical surfaces that have smaller diameters (lower radial values).

In expressions (1) through (5), the functions J_0 and J_1 are Bessel functions. When their magnitudes are plotted (as they are in figure 3) they resemble damped cosine and sine waves. This shows how the j and B variables vary with *radial distance*, r , out from the z -axis (*not* with time or distance down the axis).

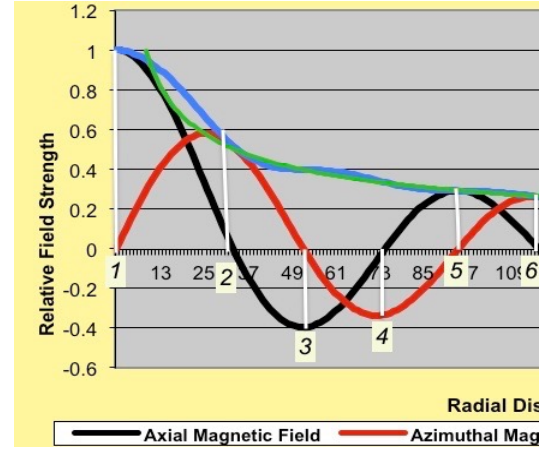


Figure 3. The vector components of j and B as functions of radius, r .

Every point, p , that lies on a virtual concentric cylinder whose radius is some specific value of r , is the origin of a pair of vectors, $B(r)$ and $j(r)$. Every one of those magnetic vectors, $B(r)$, has identical components B_z and B_θ and so all have the same angle with respect to the z and θ axes. A similar property holds for the components of each $j(r)$ vector (which is parallel to $B(r)$). Thus, each such cylindrical surface will have on its surface, an unlimited and uncountable set of parallel, **helical** vector pathways. A **helix** is a twisting curve traced on a **cylinder** by the rotation of a point crossing its cross-sections at a constant oblique angle. In contrast, a **spiral** or **vortex** is a curve traced on a **cone** by the rotation of a point crossing its cross-sections at a constant oblique angle.

At $r = 0$ (see point 1 in figure 3) B_z is at its maximum value and $B_\theta = 0$. The same holds for the components of the vector j . Thus it is clear that the parallel pair of vectors j, B is pointed directly down the z -axis at $r = 0$. As r increases, (as we get farther from the central z -axis) the magnitude of the B_z component smoothly decreases, as shown in figure 3, and the magnitude of the B_θ component increases – thereby rotating the B and j pair in the clockwise direction (Fig.1).

At the value of r where the black and red curves intersect, the pitch angle is 45° . As we move p outward, increasing its radius, r , to point 2 in figure 1, the axial component

becomes zero-valued and the wrap-around component attains its first maximum value (approximately 0.6). Therefore, at this value of r , the \mathbf{j}, \mathbf{B} pair of vectors is pointed only in the ‘wrap-around’ (azimuthal) direction. This is the point at which essentially all earlier plasma investigators have stopped trying to plot what the structure looks like. See figure 4. But it is clear from figure 3 that the Bessel functions (and therefore both the \mathbf{j} and \mathbf{B} vectors) do not stop. They continue to exist at values of r greater than that at point 2. Point 2 is not in any way an upper limit to the radial size (diameter) of the BC.

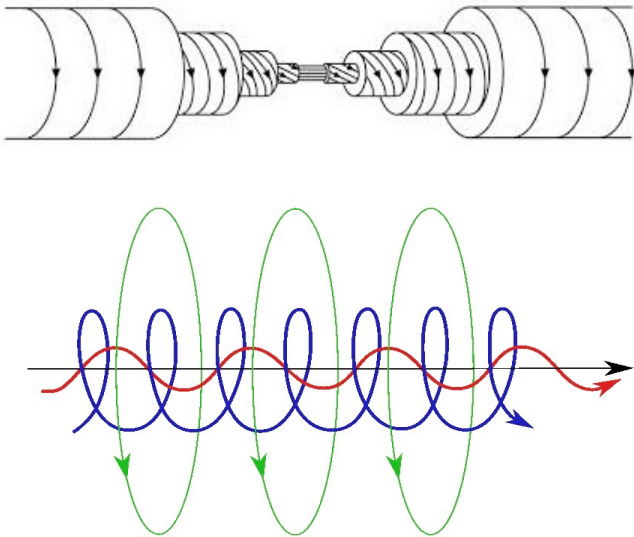


Figure 4 (Top) Cutaway diagram of a BC. (Bottom) Image used by Alfvén and many other investigators of Birkeland Currents. The outermost surface shown in both diagrams corresponds to point 2 in figure 3.

So figure 4 and others like it are misleading. The next layer (if it were added) would show a set of helical wraps coming down over the top of the cable that slope slightly toward the left.

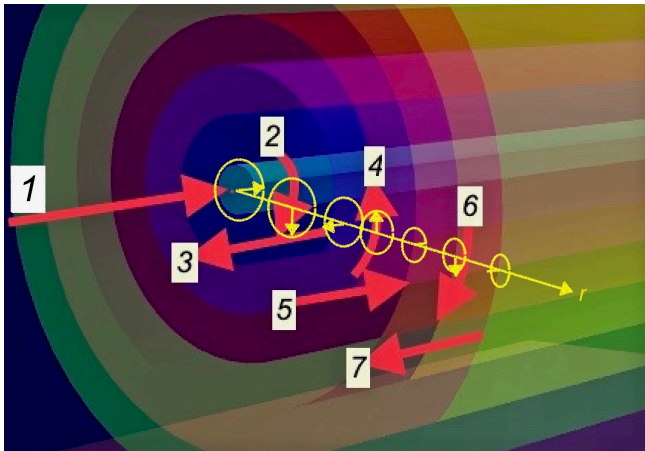


Figure 5 Showing several different virtual cylinders and the direction of the \mathbf{j}, \mathbf{B} vectors on their surfaces.

Figure 5 shows how the helical wrapping continues for values of radius, r , larger than point 2. Beyond point 2 the \mathbf{j}, \mathbf{B} vectors begin to point slightly in the negative z -direction. In this figure the z -axis is horizontal, pointing away from the viewer toward the right as shown by red arrow #1. We are at a viewpoint just above the horizontal plane, looking back toward the model, down a radial, r -axis (shown in yellow). The points numbered 1-7 correspond to those same numbers as shown in figure 3.

The yellow ‘‘clock-faces’’ in figure 5 show how the direction of the \mathbf{j}, \mathbf{B} pair of vectors rotate (clockwise in this view) at various radial distances. It is important to realize that both the magnitude (strength) of \mathbf{j} and \mathbf{B} decrease with increasing r as $1/\sqrt{r}$. This is shown by the diminishing size of the ‘‘clock-faces’’.

It must also be realized that this rotation of the \mathbf{j}, \mathbf{B} vector pairs proceeds smoothly (continuously), not in discrete jumps. Therefore the cylindrical surfaces shown in figure 5 do not exist in reality. They are *virtual surfaces* that mark important radial values – markers to indicate where one or the other components of \mathbf{j} and \mathbf{B} are zero-valued. They serve a purpose similar to the contours on a topographical map. When one views an actual mountain, the topographic contours are of course not visible. They can be added onto an image or map of the mountain to show the locus of points that have some specific identical altitude above-sea-level. A conceptual visualization aid (of the \mathbf{j}, \mathbf{B} vector pairs) might be a helically twisting swarm of insects, none of which ever collide with or diverge away from one another. The correct mathematical term for a large number of such vectors is a ‘‘vector-field’’.

With reference to figure 5, we note, for example, that at point 2, (call this radius value $r = r_{p2}$) the vector pair are pointed downward (in the 6 o’clock direction). An incremental radial distance farther out, at $r = r_{p2} + \Delta r$, the angle has shifted clockwise toward the 7 o’clock direction. (This is also shown in figure 7.)

IV. CONTRASTING PROPERTIES OF \mathbf{J} AND \mathbf{B}

The two state variables that are modeled in this study of a force-free current (FFC) are:

- 1) The current density, $\mathbf{j}(r)$, and
- 2) The magnetic field strength, $\mathbf{B}(r)$.

These both have identically shaped vector fields. They are parallel (coincident) at every point within the body of the FFC and their magnitudes are proportional to each other.

But, their differences are important. Maxwell’s equations show that electric currents cause magnetic fields. But, it is *not correct* that the current density vector, $\mathbf{j}(p)$, at any given single point, p , is the sole cause of the magnetic-field, $\mathbf{B}(p)$ at that same location. Actually the value of $\mathbf{B}(p)$ is the result of a sum¹ (integral) of the effects of *every* $\mathbf{j}(p)$ vector in that region.

¹ Stokes theorem.

Whereas the current density vector stream is made up of an actual *flow* of moving individual charges, there is nothing flowing along the magnetic-field \mathbf{B} -vector. It does not consist of a stream of particles. The magnetic field vector does not imply motion of any kind. Faraday’s invention of magnetic-field “lines” that are labeled with directional arrows (and the practice of calling a magnetic-field a *flux*) has led to many misinterpretations of what is actually occurring in a magnetic field. Nothing moves along the \mathbf{B} -vector. Its direction simply indicates the direction in which a tiny magnetic test compass would point if inserted into the field at that location.

On the other hand, current density streams are indeed collections of moving charged particles which can often interact with each other. They are subject to temperature driven random motion. In addition, the current density vector can be physically diverted by an externally applied electric-field, \mathbf{E} . But, magnetic-fields, \mathbf{B} , are unaffected by steady-state \mathbf{E} -fields. Also because they do not consist of moving particles, \mathbf{B} -fields are not subject to temperature induced random distortions or collisions.

We conclude from the above that the \mathbf{B} -field is less likely to suffer any kind of perturbation caused by accidentally encountered causes than is the current density vector, $\mathbf{j}(r)$.

V. SELF-ORGANIZING AND SELF-SUSTAINING

The first two paragraphs of the introduction (section I) delineate the fundamental assumptions on which the Bessel function model was derived: Eliminate all external forces, and allow a moving cloud of charges (a plasma) to form itself into whatever shape it naturally collapses. That final, freely formed structure is surprisingly complex – but it is clearly a self-organized minimum energy structure. Its precise shape is derived by seeking a structure within which the inherent magnetic Lorentz forces are zero-valued everywhere in the plasma.

Is there a specific property of the Bessel function model that explains why FFCs keep their form over extremely long inter-galactic distances? There are diffusible electrostatic repelling forces among all like particles inside a BC: all the like-charges push away from each other. There is no way to prevent that even after we have eliminated all the Lorentz forces by making the \mathbf{j} and \mathbf{B} vectors at every point parallel. So what about those mutually repellant electrostatic forces? Also, it has been suggested [1], that a constant \mathbf{E} -field extends radially outward from the z -axis. That, additional to the mutually repellant forces, pushes positive charges outward away from the z -axis. So there is an inherent tendency for the BC to expand outward radially. Why doesn’t it?

A clue to the answer to this question is provided by the last sentence in the previous section: “the \mathbf{B} -field is much less likely to suffer any kind of perturbation caused by accidentally encountered causes than is the current density

vector, $\mathbf{j}(r)$.” Before any change can occur in the magnetic flux density vector field, \mathbf{B} , a change must take place in the current density, \mathbf{j} .

For example, suppose that a single positively charged particle in the \mathbf{j} vector stream becomes accidentally dislocated outward to a larger value of radius, r . This perturbation places it in a region of slightly rotated \mathbf{B} -field. (See the last paragraph in section 3.) A Lorentz magnetic force arises on the errant particle in the negative r direction. This tends to restore it to its proper position. No matter whether the perturbation of the \mathbf{j} vector is inward (toward the z -axis, or outward, the resulting Lorentz force will be in the restorative direction. This example is illustrated in figure 7.

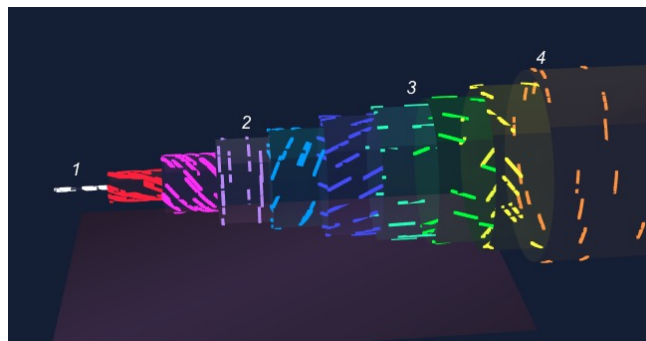


Figure 6 Several discrete virtual cylindrical surfaces. Each is the location of \mathbf{jB} vector pairs having pitch angles that increase with radial value, r . This is a detailed version of the right half of the top of figure 4. Numbers correspond to radial values shown in figures 3 and 5.

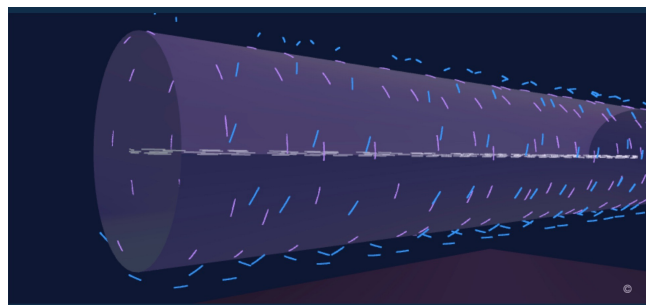


Figure 7 Two closely-spaced radial values. The inner cylinder shows the azimuthal \mathbf{jB} vector pairs that occur at point 2 in figures 3, 5 and 6. Just above that radius, the vectors have rotated slightly clockwise (in this view).

In figure 7 the inner cylinder contains \mathbf{jB} vectors corresponding to point 2 in figures 3, 5 and 6. At that radius they are completely azimuthal (no z -axial component). Just above them (at radius $r = r_{p2} + \Delta r$) the vector pairs have rotated slightly toward the seven o’clock direction. If a \mathbf{j} vector becomes displaced outward from the inner cylinder, it will intersect the slightly rotated \mathbf{B} vector. The resulting Lorentz force, $\mathbf{f}_L = \mathbf{j} \times \mathbf{B}$, will be in the negative r direction, thus restoring the \mathbf{j} vector to its original location.

This *negative-feedback mechanism operates at every location within the plasma* (not just at its outer surface). This is an inherent consequence of the unique, complex, Bessel function shape of the FFC. It maintains the integrity of the structure in exact conformity with the model (expressions 1 – 5 in section 3).

The model clearly represents a minimum-energy system. Any perturbation of it, by definition, is a non-minimum energy system which naturally will revert to its minimum-energy form if it is allowed to do so. A Force-Free current is thus both *self-organizing* and *self-sustaining*.

VI. FORCE-FREE VS BIRKELAND CURRENTS

The primary goal of this paper is to provide an intuitive understanding of the physical shape of a FFC and the consequences of that shape. Section III contained a statement defining the difference between a *helix* and a *spiral*. The helix is formed by wrapping something around a cylinder – thus it has a constant diameter that does not vary with distance down its axis. The spiral is a tapered form – a vortex. Its diameter becomes smaller with distance along its axis. A force-free current has a helix shape as it travels undisturbed through space. But when it encounters an external force or obstruction such as the magnetosphere of a planet or a ‘z-pinch’, its diameter often becomes reduced. Such constrictions cause the current density to increase (same total current – reduced cross-section) which, in turn, may cause matter to collect in zones within the cross-section of the current [1] and also can change the plasma from dark to glow or arc mode. This is what occurs in Birkeland Currents. So, a Force-Free Current is the canonical (purest) form and the Birkeland Current is a modified form of this cosmic transport channel.

VII. CONCLUSION

The simplest description of the structure of a FFC is that it consists of an unbounded and uncountable set of two vector-field quantities (magnetic-field, \mathbf{B} , and current density, \mathbf{j}) that form on virtual concentric cylindrical surfaces that are incrementally separated by a radial differential element, dr . On each of these concentric surfaces the vector quantities form parallel (non-intersecting) helixes, and their direction (‘pitch-angle’) differs incrementally (from the vector set on the virtual cylinder immediately below them). This results in a continually smooth variation in pitch of the helixes with increasing radius, r . This variation in pitch angle enables a potentially restoring Lorentz force to maintain a robust structure. This explains the amazing longitudinal stability of cometary and stellar jets, some of which are observed to be many light-years in length.

VIII. TABLE I

Column 1 = “Points” listed in figures 3, 5, and 6.
 Columns 2 & 3 = Independent variable, x , values of zeros of Bessel functions $J_0(x)$ and $J_1(x)$.
 Column 4 = Maximum and zero values of \mathbf{B} and \mathbf{j} .

Point #	x	x	Event
1		0	B_z pos max, B_θ zero.
2	2.4048		B_z zero, B_θ pos max
3		3.8317	B_z neg max, B_θ zero
4	5.5201		B_z zero, B_θ neg max
5		7.0156	B_z pos max, B_θ zero
6	8.6537		B_z zero, B_θ pos max
7		10.1735	B_z neg max, B_θ zero.
8	11.7915		B_z zero, B_θ neg max
9		13.3237	B_z pos max, B_θ zero
10	14.9309		B_z zero, B_θ pos max

IX. ACKNOWLEDGEMENT

Figures 5, 6, and 7 are contributed by James Sorensen of *etherealmatters.com* without whose help and continued efforts they would not exist. He has developed simulation software that allows 3D views of the FFC structure that can be manipulated by the viewer to show continuously changing orientations of the model. The number, density and intensity of various virtual cylinders and incremental (particle) vectors can also be controlled by the viewer. The images included here are screen-shots of his program in action.

X. REFERENCES

- [1] Scott, D. A Force-Free Field-Aligned Model. Prog. Phys., 2015, v. 10(1), 167–178 <http://www.ptep-online.com/2015/PP-41-13.PDF>
- [2] Scott, D. Birkeland Currents and Dark Matter. Prog. Phys., 2018, v. 14(2), 57–62 <http://www.ptep-online.com/2018/PP-53-01.PDF>
- [3] Lundquist S. Magneto-Hydrostatic Fields Arch. Fys. 2, 361, 1950.
- [4] Lundquist S. On the Stability of Magneto-Hydrostatic Fields Phys. Rev. Vol. 83 issue 2 p. 307-311, 1951. Available: <http://link.aps.org/doi/10.1103/PhysRev.83.307>